Photochemical Activation of Ruthenium(II)−Pyridylamine Complexes Having a Pyridine-N-Oxide Pendant toward Oxygenation of Organic Substrates

Takahiko Kojima,*,[†] Kazuya Nakayama,[‡] Miyuki Sakaguchi,[¶] Takashi Ogura,[¶] Kei Ohkubo,[‡,⊥] and Shunichi Fukuzumi*,[‡,§,⊥]

[†]Department of Chemistry, Graduate School of Pure and Applied Sciences, University of Tsukuba, 1-1-1 Tennoudai, Tsukuba, Ibaraki 305-8571, Japan

[‡]Department of Material and Life Science, Graduate School of Engineering, Osaka University, and [⊥]ALCA, Japan Science and Technology Agency (JST), 2-1 Yamada-oka, Suita, Osaka 565-0871, Japan

[¶]Graduate School of Life Science, University of Hyogo, Kouto, Hyogo 678-1297, Japan

[§]Department of Bioinspired Science, Ewha Womans University, Seoul 120-750, South Korea

S *Supporting Information*

ABSTRACT: Ruthenium(II)−acetonitrile complexes having η^3-tris(2-pyridylmethyl)amine (TPA) with an uncoordinated pyridine ring and diimine such as 2,2′-bipyridine (bpy) and 2,2′-bipyrimidine (bpm), $[Ru^{II}(\eta^3\text{-TPA})(\text{diimine})(CH_3CN)]^{2+}$, reacted with m-chloroperbenzoic acid to afford corresponding Ru(II)−acetonitrile complexes having an uncoordinated pyridine-N-oxide arm, $[Ru^{II}(\eta^3\text{-TPA-O})(\text{diimine})(CH_3CN)]^{2+}$, with retention of the coordination environment. Photoirradiation of the acetonitrile complexes having diimine and the η^3-TPA with the uncoordinated pyridine-N-oxide arm afforded a

mixture of $[Ru^{II}(TPA)(\text{diimine})]^{2+}$, intermediate-spin $(S = 1)$ Ru(IV)−oxo complex with uncoordinated pyridine arm, and intermediate-spin Ru(IV)−oxo complex with uncoordinated pyridine-N-oxide arm. A Ru(II) complex bearing an oxygen-bound pyridine-N-oxide as a ligand and bpm as a diimine ligand was also obtained, and its crystal structure was determined by X-ray crystallography. Femtosecond laser flash photolysis of the isolated O-coordinated Ru(II)−pyridine-N-oxide complex has been investigated to reveal the photodynamics. The Ru(IV)−oxo complex with an uncoordinated pyridine moiety was alternatively prepared by reaction of the corresponding acetonitrile complex with 2,6-dichloropyridine-N-oxide (Cl$_2$py-O) to identify the Ru(IV)−oxo species. The formation of Ru(IV)−oxo complexes was concluded to proceed via intermolecular oxygen atom transfer from the uncoordinated pyridine-N-oxide to a Ru(II) center on the basis of the results of the reaction with Cl$_2$py-O and the concentration dependence of the consumption of the starting Ru(II) complexes having the uncoordinated pyridine-N-oxide moiety. Oxygenation reactions of organic substrates by $[Ru^{II}(\eta^3\text{-TPA-O})(\text{diimine})(CH_3CN)]^{2+}$ were examined under irradiation (at 420 ± 5 nm) and showed selective allylic oxygenation of cyclohexene to give cyclohexen-1-ol and cyclohexen-1-one and cumene oxygenation to afford cumyl alcohol and acetophenone.
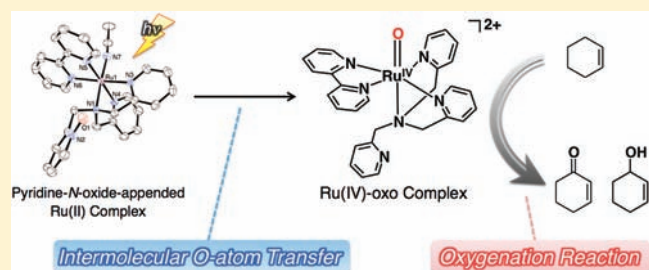
■ INTRODUCTION

In the course of the oxidative conversion of organic substrates, high-valent transition metal−oxo complexes play a pivotal role as responsible species of the reactions.[1−6] Not only substrate oxidation with high-valent metal−oxo complexes to afford oxidized products[7−9] but also formation of the high-valent metal−oxo complexes have been intensively investigated to elucidate activation mechanisms of oxidants at the metal centers.[8−11] The high-valent metal−oxo complexes have been formed mainly by reactions of metal complexes through dioxygen activation,[12−14] with active oxygen species such as peroxides[4,15−18] and iodosylarenes,[19] and also through proton-coupled electron-transfer oxidation.[20] On the other hand, photochemical formation of high-valent metal−oxo

complexes has been investigated for use in substrate oxygenation using metal−porphyrin complexes via homolytic cleavage of the Cl−O bond in coordinated ClO$_4^-$ by laser flash photolysis.[21]

As a strategy for the formation of reactive species in metal-catalyzed oxidation reactions, pyridine-N-oxides, such as 2,6-dichloropyridine-N-oxide, have been adopted as terminal oxidants, especially for ruthenium complexes as catalysts.[22,23] A benefit to use of pyridine-N-oxides as oxidants is the prevention of radical chain reactions that may result in complicated reaction pathways affording less-selective formation of oxidation products. As a
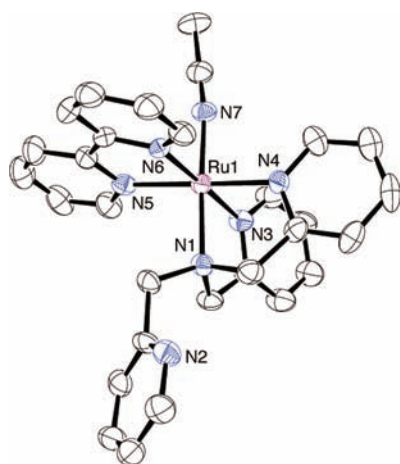
Scheme 1

Figure 1. ORTEP drawing of the cation part of **2a** with partial numbering scheme (50% probability thermal ellipsoids). Hydrogen atoms are omitted for clarity. Selected bond lengths (Å) and angles (deg): Ru1−N1 2.115(5), Ru1−N3 2.053(5), Ru1−N4 2.083(5), Ru1−N5 2.057(5), Ru1−N6 2.072(6), Ru1−N7 2.011(5); N1−Ru1−N3 81.9(2), N1−Ru1−N4 81.4(2), N3−Ru1−N4 81.8(2), N5−Ru1−N6 78.9(2).
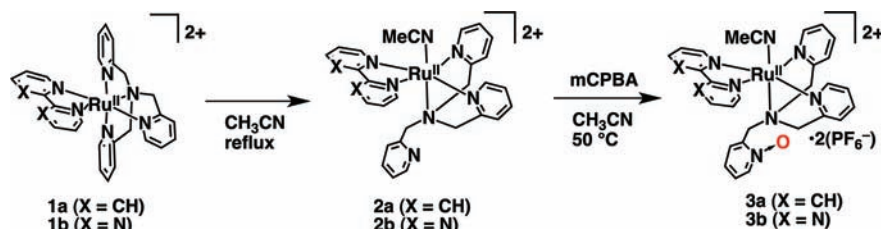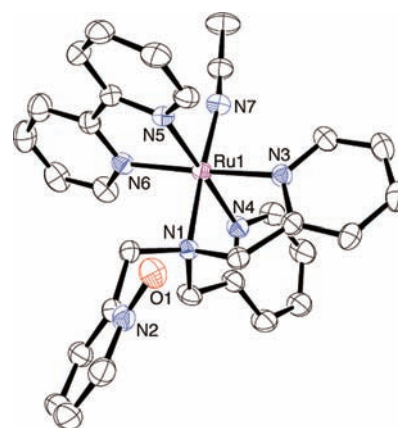
Figure 2. ORTEP drawing of the cation part of **3a** with partial numbering scheme (50% probability thermal ellipsoids). Hydrogen atoms are omitted for clarity. Selected bond lengths (Å) and angles (deg): Ru1−N1 2.123(2), Ru1−N3 2.050(3), Ru1−N4 2.078(3), Ru1−N5 2.054(3), Ru1−N6 2.074(3), Ru1−N7 2.031(2), O1−N2 1.309(4); N1−Ru1−N3 81.93(10), N1−Ru1−N4 80.86(11), N3−Ru1−N4 82.25(12), N5−Ru1−N6 78.77(13).

milder oxidant, pyridine-*N*-oxides have been reported to be essential for selective oxidation processes.[24] The reactions of pyridine-*N*-oxides with metal complexes, which require photoirradiation, have been proposed to afford high-valent metal−oxo complexes as reactive species in catalytic oxidation reactions.[22] Such photochemical reactions with mild oxidants such as pyridine-*N*-oxides would provide versatile pathways to produce high-valent metal−oxo complexes. However, there has been no report on the direct detection or isolation of high-valent metal−oxo complexes in photochemical reactions of metal complexes with mild oxidants.

We report herein photochemical formation of high-valent metal−oxo complexes for the first time by using a Ru(II)−diimine complex having an uncoordinated pyridine-*N*-oxide arm (TPA-O) derived from the η^3-tris(2-pyridylmethyl)amine (TPA) ligand, $[Ru^{II}(\eta^3\text{-TPA-O})(\text{diimine})(CH_3CN)]^{2+}$, which has been newly synthesized and structurally characterized by X-ray crystallography. The photochemical formation of Ru(IV)−oxo complexes together with the *O*-coordinated Ru(II)−pyridine-*N*-oxide complex, derived from $[Ru^{II}(\eta^3\text{-TPA-O})(\text{diimine})(CH_3CN)]^{2+}$, was compared with the photochemical reaction of $[Ru^{II}(\eta^3\text{-TPA})(\text{diimine})(CH_3CN)]^{2+}$ without an uncoordinated pyridine-*N*-oxide arm with an external oxidant, 2,6-dichloropyridine-*N*-oxide. The oxygenation of substrates with $[Ru^{II}(\eta^3\text{-TPA-O})(\text{diimine})(CH_3CN)]^{2+}$ under photoirradiation

was also investigated to clarify the oxidizing ability of the photogenerated Ru(IV)−oxo complex.

■ RESULTS AND DISCUSSION

Reaction of *m*-Chloroperbenzoic Acid To Form Ru(II) Complexes with Pyridine-*N*-Oxide Arm. Ru(II)-TPA-diimine complexes, $[Ru(TPA)(\text{diimine})](PF_6)_2$ (diimine = 2,2′-bipyridine (bpy, **1a**); 2,2′-bipyrimidine (bpm, **1b**)), undergo a complete thermal structural change in CH_3CN to give $[Ru(\eta^3\text{-TPA})(\text{diimine})(CH_3CN)](PF_6)_2$ (diimine = bpy (**2a**); bpm (**2b**)), in which the TPA ligand binds to the Ru(II) center as a tridentate ligand in a *facial* configuration with an uncoordinated pyridine arm.[25] The reaction of *m*-chloroperbenzoic acid (*m*CPBA) with **2a** and **2b** gave complexes bearing a uncoordinated pyridine-*N*-oxide arm, $[Ru(\eta^3\text{-TPA-O})(\text{diimine})(CH_3CN)](PF_6)_2$ (diimine = bpy (**3a**); bpm (**3b**)), as described in Scheme 1. The second-order rate constant for the reaction of **2a** with *m*CPBA to form **3a** was determined to be $(1.45 \pm 0.16) \times 10^{-2}$ M^{-1} s^{-1} in CH_3CN at 323 K (Figure S1 in the Supporting Information (SI)). The oxidation state of the ruthenium center remains +2, even in the presence of an excess amount of *m*CPBA.

The crystal structure of **2a** was determined by X-ray crystallography. Its ORTEP drawing is depicted in Figure 1 involving partial numbering scheme with 50% thermal ellipsoids and selected bond lengths and angles are given in the figure caption. It is clear

that this complex has an uncoordinated pyridine moiety and an acetonitrile ligand. The TPA ligand acts as a *facial* tridentate ligand in sharp contrast to that in **1**, in which TPA binds to the Ru(II) center as a tetradentate ligand. The bond length of Ru1–N7-(acetonitrile) is 2.011(5) Å, which is the shortest coordination bond in **2a**. This strong interaction causes elongation of the bond length of Ru1–N1(*tert*-amino nitrogen) to be 2.115(5) Å, due to the *trans* influence of the acetonitrile ligand.

X-ray crystallography on **3a** allowed us to access a unique structure involving an uncoordinated pyridine-*N*-oxide moiety. So far, no example has been reported on a metal complex bearing an uncoordinated pyridine-*N*-oxide moiety. An ORTEP drawing of the cation part of **3a** is shown in Figure 2, involving numbering scheme with 50% probability thermal ellipsoids, and selected bond lengths and angles are given in the figure caption. In this complex, the TPA ligand maintains a facial tridentate coordination mode and the nitrogen atom of the uncoordinated pyridine pendant is oxygenated by *m*CPBA to give rise to an uncoordinated pyridine *N*-oxide moiety. The bond length of Ru1–N7-(acetonitrile) is shortest to be 2.031(2) Å and the Ru1–N1(*tert*-amino nitrogen) bond is elongated to be 2.123(2) Å as well as that in **2a**. The bond length of N(2)–O(1) of the *N*-oxide is 1.309(4) Å.

In the absorption spectra of **3a** and **3b** in CH_3CN, no significant change was observed in comparison with those of **2a** and **2b** (Figure S2 in SI). In the NMR spectra of **3a** and **3b** in CD_3CN, a downfield shift was observed for a doublet due to the methylene group of a coordinating pyridylmethyl arm (Figures S3

and S4 in SI). In the ESI-MS spectrum, the *N*-oxide-appended complexes **3a** and **3b** exhibited peak clusters at $m/z = 750.1$ for **3a** ($\{[Ru(\eta^3\text{-TPA-O})(bpy)(CH_3CN)](PF_6)\}^+$) and at $m/z = 752.1$ for **3b** ($\{[Ru(\eta^3\text{-TPA-O})(bpm)(CH_3CN)](PF_6)\}^+$) as shown in Figure 3.

Photochemical Reactions of Ruthenium Complexes Having Pyridine-*N*-Oxide Pendant. Photoirradiation of complexes **3a** at 420 nm and **3b** at 450 nm in CD_3CN at room temperature resulted in formation of the *O*-coordinated Ru(II)−pyridine-*N*-oxide complex ($[(Ru\text{-O-TPA})(bpm)](PF_6)_2$ **4b**) and Ru(IV)−oxo complexes, $[Ru(O)(TPA)(diimine)](PF_6)_2$ (**5a** with bpy and **5b** with bpm), and small amount of Ru(IV)−oxo complexes with uncoordinated pyridine-*N*-oxide pendant, $[Ru(O)(\eta^3\text{-TPA-O})(diimine)](PF_6)_2$ (**6a** for bpy and **6b** for bpm), as well as **1a** and **1b** as shown in Scheme 2. The identification of each product in Scheme 2 is described below. As for the bpy complex **3a**, the corresponding *O*-coordinated Ru(II)−pyridine-*N*-oxide complex, $[(Ru\text{-O-TPA})(bpy)](PF_6)_2$ (**4a**), was not detected by ^1H NMR spectrometry, in contrast to the case of **3b** to from **4b**.

In the ESI-MS spectrum of the reaction mixture including **3b** with bpm under photoirradiation at 450 nm in CD_3CN (Figure 4), we could observe a peak cluster (◆) assignable to both pyridine-*N*-oxide-coordinated $\{[(Ru\text{-O-TPA})(bpm)]-(PF_6)\}^+$ ($\{4b − (PF_6)\}^+$) and the Ru(IV)−oxo complex
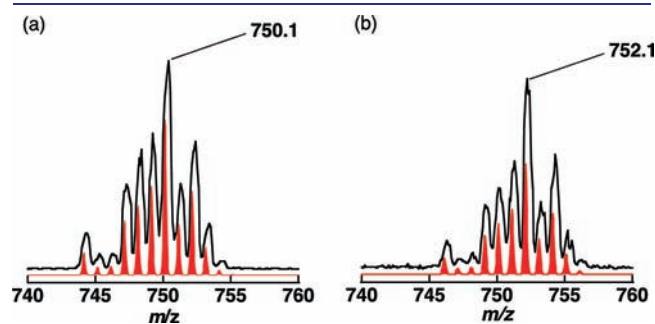

Figure 3. ESI-MS spectra of **3a** (a) and **3b** (b). The red lines are simulated isotopic patterns.

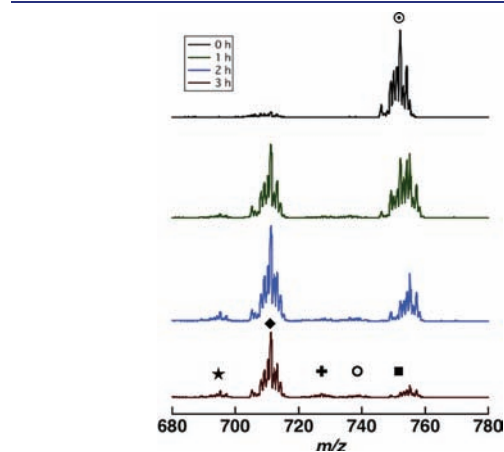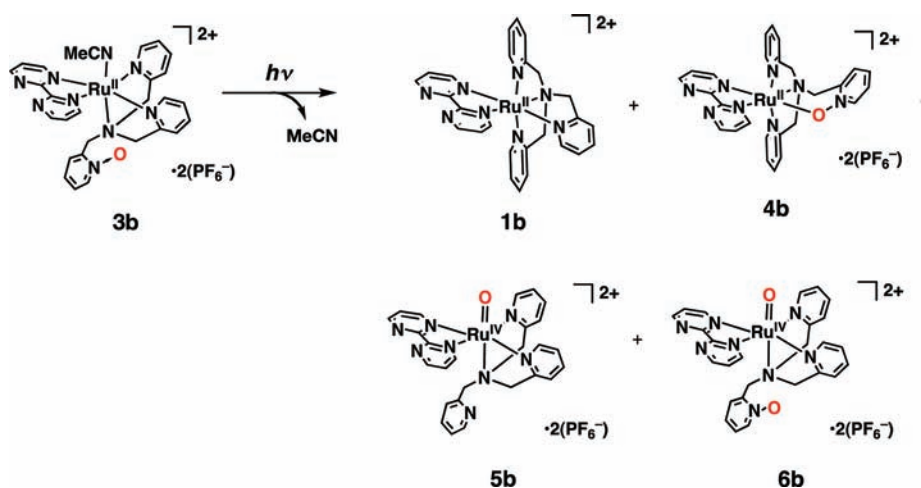

Figure 4. Time course of ESI-MS spectra of **3b** under photoirradiation at 450 nm in CD_3CN.
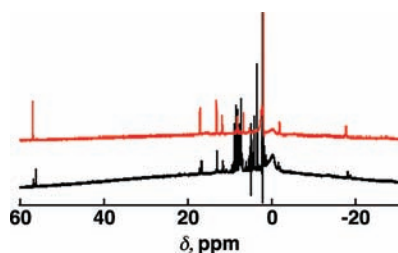
Scheme 2

Figure 5. ^{1}H NMR spectra of a solution containing $[\mathrm{Ru^{IV}(O)}(\eta^3\text{-}\mathrm{TPAH^+})(\mathrm{bpy})](\mathrm{PF_6})_3$ (5 mM) formed by oxidation of **1a** by CAN in $\mathrm{CD_3CN}$ at room temperature (red trace) and the solution of **3a** (5 mM) after photoirradiation at 420 nm for 3 h in $\mathrm{CD_3CN}$ at room temperature (black trace).

Figure 6. ^{1}H NMR spectra of a solution containing $[\mathrm{Ru^{IV}(O)}\text{-}(\mathrm{H^+TPA})(\mathrm{bpm})](\mathrm{PF_6})_3$ (5 mM) formed by oxidation of **1b** by CAN in $\mathrm{CD_3CN}$ at room temperature (red trace) and the solution of **3b** (5 mM) after photoirradiation at 450 nm for 3 h in $\mathrm{CD_3CN}$ at room temperature (black trace).

$\{[\mathrm{Ru(O)}(\eta^3\text{-}\mathrm{TPA})(\mathrm{bpm})](\mathrm{PF_6})\}^+$ at $m/z = 711.1$ ($\{\mathbf{5b} - (\mathrm{PF_6})\}^+$) as main products. As a minor peak cluster, at $m/z = 727.1$ is assigned to $\{[\mathrm{Ru(O)}(\eta^3\text{-}\mathrm{TPA\text{-}O})(\mathrm{bpm})](\mathrm{PF_6})\}^+$ ($+$, $\{\mathbf{6b} - (\mathrm{PF_6})\}^+$). The isotopic patterns of those peak clusters are consistent with simulated patterns as shown in Figure S5 (SI). In addition, small peak clusters due to $\{[\mathrm{Ru(TPA)(bpm)}](\mathrm{PF_6})\}^+$ at $m/z = 695.1$ ($\star$, $\{\mathbf{1b} - (\mathrm{PF_6})\}^+$) and $\{[\mathrm{Ru}(\eta^3\text{-}\mathrm{TPA})\text{-}(\mathrm{CD_3CN})(\mathrm{bpm})](\mathrm{PF_6})\}^+$ at $m/z = 739.1$ ($\bigcirc$, $\{\mathbf{2b} - (\mathrm{PF_6})\}^+$) were observed at the end of the reaction. The peak due to the starting $\{[\mathrm{Ru}(\eta^3\text{-}\mathrm{TPA\text{-}O})(\mathrm{CH_3CN})(\mathrm{bpm})](\mathrm{PF_6})\}^+$ at $m/z = 752.1$ ($\odot$, $\{\mathbf{3b} - (\mathrm{PF_6})\}^+$) lowered its intensity and shifted to that due to $\{[\mathrm{Ru}(\eta^3\text{-}\mathrm{TPA\text{-}O})(\mathrm{CD_3CN})(\mathrm{bpm})](\mathrm{PF_6})\}^+$ at $m/z = 755.1$ ($\blacksquare$, $\{\mathbf{3b} - (\mathrm{PF_6})\}^+$) because of photoinduced ligand substitution of $\mathrm{CH_3CN}$ by the deuterated solvent, $\mathrm{CD_3CN}$.

The formation of **1b** and **6b** in Scheme 2 suggests that an oxo transfer reaction occurs between two molecules of **3b**. ESI-MS measurements on **3a** under photoirradiation at 420 nm in $\mathrm{CD_3CN}$ allowed us to observe peak clusters assigned to $\{[\mathrm{Ru(O)}(\eta^3\text{-}\mathrm{TPA})(\mathrm{bpy})](\mathrm{PF_6})\}^+$ ($\{\mathbf{5a} - (\mathrm{PF_6})\}^+$) at $m/z = 709.1$, $\{[\mathrm{Ru(O)}(\eta^3\text{-}\mathrm{TPA\text{-}O})(\mathrm{bpy})](\mathrm{PF_6})\}^+$ ($\{\mathbf{6a} - (\mathrm{PF_6})\}^+$) at $m/z = 725.1$, $\{[\mathrm{Ru(TPA)(bpy)}](\mathrm{PF_6})\}^+$ ($\{\mathbf{1a} - (\mathrm{PF_6})\}^+$) at $m/z = 693.1$ and $\{[\mathrm{Ru}(\eta^3\text{-}\mathrm{TPA})(\mathrm{bpy})(\mathrm{CD_3CN})](\mathrm{PF_6})\}^+$ ($\{\mathbf{2a} - (\mathrm{PF_6})\}^+$) at $m/z = 737.1$ (Figures S6 and S7 in SI). In the NMR spectrum, signals assigned to those of **1a** were detected, however, no signals due to the O-coordinated Ru(II)−pyridine-N-oxide complex (**4a**) were observed in $\mathrm{CD_3CN}$. This is probably due to stronger interaction of the N-oxide oxygen with the Ru(II) center of **4b** than that in **4a**: The pyrimidine may act as a better π-acceptor for the π-back bonding than pyridine to enhance the electron donation from the N-oxide oxygen as a π-donor to strengthen the interaction.[20] In addition, the difference may stem from that of the quantum yields of the coordination of the N-oxide oxygen via the release of $\mathrm{CH_3CN}$. The quantum yields of the reaction from **2** to **1** have been determined to be 0.0057 for **2a** and 0.028 for **2b**, and those of the reverse reaction (**1** to **2**) have been reported to be 0.0021 for **1a** and 0.0017 for **1b**.[25a] Thus, more efficient structural change can be expected for **2a** to consume **4a** for further reactions.

In the ^{1}H NMR spectra of photoirradiated solutions of **3a** and **3b**, paramagnetically shifted signals were observed in the range of 60 to −20 ppm. Photoirradiation of **3a** at 420 nm in $\mathrm{CD_3CN}$ gave rise to two sets of paramagnetically shifted peaks, suggesting one major and one minor products, as can be seen in the black trace in Figure 5. The chemical shifts of those signals are consistent with or close to those for a crystallographycally characterized intermediate-spin ($S = 1$) Ru(IV)−oxo complex, $[\mathrm{Ru^{IV}(O)}(\eta^3\text{-}$

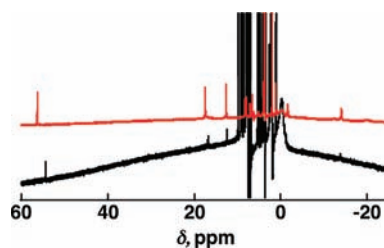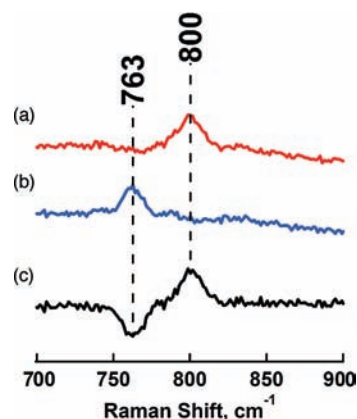**Figure 7.** Resonance Raman spectra of $[\mathrm{Ru}(^{16}\mathrm{O})(\eta^3\text{-}\mathrm{TPAH^+})(\mathrm{bpm})]^{3+}$ (a), $[\mathrm{Ru}(^{18}\mathrm{O})(\eta^3\text{-}\mathrm{TPAH^+})(\mathrm{bpm})]^{3+}$ (b), and their differential spectrum ($^{16}\mathrm{O} - {}^{18}\mathrm{O}$) (c).

$\mathrm{TPAH^+})(\mathrm{bpy})]^{3+}$.[26] Thus, we concluded that the photoirradiation of **3a** can afford two kinds of Ru(IV)−oxo complexes in the $S = 1$ spin state. As for **3b**, the spectrum of the photoproduct (black trace in Figure 6) was similar to that (red trace in Figure 6) of $[\mathrm{Ru(O)}(\eta^3\text{-}\mathrm{TPAH^+})(\mathrm{bpm})]^{3+}$, which was formed by the reaction of **1b** with $(\mathrm{NH_4})_2[\mathrm{Ce^{IV}(NO_3)_6}]$ (CAN) in water. In the resonance Raman spectrum of $[\mathrm{Ru(O)}(\eta^3\text{-}\mathrm{TPAH^+})(\mathrm{bpm})]^{3+}$, a Raman scattering due to the Ru=O moiety was observed at 800 cm^{-1} (Figure 7(a)), which was close to those of $[\mathrm{Ru^{IV}(O)}(\eta^3\text{-}\mathrm{TPAH^+})(\mathrm{bpy})]^{3+}$ (805 cm^{-1})[25] and $[\mathrm{Ru^{IV}(O)(TPA)(OH_2)}]^{2+}$ (806 cm^{-1}).[27] The peak shifted to 763 cm^{-1} (Figure 7(b)) by using $\mathrm{H_2}^{18}\mathrm{O}$ as a solvent to generate the Ru(IV)−oxo complex; the isotope shift is consistent with the calculated value ($\Delta\nu = 40$ cm^{-1}) as shown in Figure 7(c). The ^{1}H NMR spectrum of **5b** was identical to that of $[\mathrm{Ru(O)}(\eta^3\text{-}\mathrm{TPAH^+})(\mathrm{bpm})]^{3+}$, supporting the formation of **5b** in the photoreaction of **3b**. Thus, we concluded that the Ru(II)-diimine complexes having the pyridine-N-oxide pendant, **3a** and **3b**, can be converted to the corresponding intermediate-spin Ru(IV)−oxo complexes by means of photoirradiation. This is the first confirmation of the photochemical formation of high-valent Ru−oxo complexes with use of pyridine-N-oxides as oxygen sources.

Concerning the O-coordinated Ru(II)−pyridine-N-oxide complex, we could obtain a single crystal of **4b** to determine its crystal structure. As depicted in Figure 8, the oxygen atom of the pyridine-N-oxide arm coordinates to the Ru(II) center to form

a six-membered chelate ring. This is the first example of a structurally characterized ruthenium complex having a pyridine-N-oxide as a ligand. The bond length of Ru1−O1 was 2.083(3) Å and the bond angle of Ru1−O1−N2 was 115.4(2)°. The bond length of O1−N2 was 1.323(5) Å, which was a little longer than that of the uncoordinated pyridine-N-oxide moiety in **3b**; it was also comparable to those of terminal and bridging pyridine-N-oxide ligands in the first-row transition metal complexes reported so far.[28]

Pyridine-N-oxides have been known as oxygen atom donors to perform catalytic oxidation of organic substrates in the presence of Ru(II) complexes under photoirradiation.[22] The reaction mechanism has been proposed to involve the coordination of the N-oxide followed by the formation of putative high-valent ruthenium-oxo complexes as reactive species.[22b]
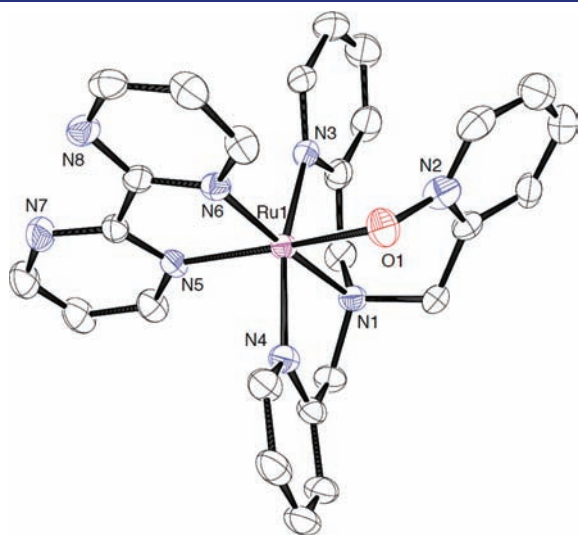

Figure 8. ORTEP drawing of the cation part of **4b** with partial numbering scheme (50% probability thermal ellipsoids). Hydrogen atoms are omitted for clarity. Selected bond lengths (Å) and angles (deg): Ru1−O1 20.84(3), Ru1−N1 2.081(2), Ru1−N3 2.069(3), Ru1−N4 2.056(3), Ru1−N5 2.091(3), Ru1−N6 2.047(3), O1−N2 1.323(5); O1−Ru1−N1 89.13(12), N1−Ru1−N3 81.72(14), N1−Ru1−N4 81.24(13), N5−Ru1−N6 78.38(12).

Therefore, we examined the conversion of **4b** to a high-valent ruthenium−oxo complex. Contrary to our expectation, the complex **4b** was consumed very slowly under photoirradiation and was intact upon heating and was proved to be stable under catalytic conditions.

In order to understand the photostability of **4b**, femtosecond laser flash photolysis of **4b** in CH_3CN was examined by photoexcitation at 420 nm to observe transient absorption spectra as shown Figure 9a. Analysis of the time-course of absorbance at 510 nm by using double-exponential curve-fitting (Figure 9b) allowed us to reveal two-step very fast reaction processes showing first-order rate constants of 2.5×10^{10} s^{-1} $((40 \text{ ps})^{-1})$ and 1.1×10^9 s^{-1} $((930 \text{ ps})^{-1})$. These two processes can be ascribed to the N−O bond cleavage and its recombination, respectively, suggesting a very short lifetime of the corresponding Ru−oxo complex (**5b**) formed from the photoreaction of **4b**. Thus, we ruled out the participation of **4b** as an intermediate for the oxidation of substrates by **3b**.

Photoirradiation of the solutions of **3** in CH_3CN allowed us to observe complicated change of absorption spectra. Therefore, the reactions were followed by ^1H NMR spectroscopy to observe change of peak integration. The spectral change was assigned to the consumption of **3** to form **1**, **2**, and **5** and/or **6**. As mentioned above, in addition to those complexes, the formation of the closed N-oxide complex **4b** was observed for **3b**. The complex **1** has been demonstrated to exhibit photochromic structural change to reach a photostationary state involving **2**.[25] The initial decay rates (bpy for 100 min and bpm for 80 min) of **3** determined by NMR measurements were revealed to show linear correlations to the initial concentration of **3** as depicted in Figure 10. This result also indicates that the consumption of **3** occurs intermolecular reactions rather than intramolecular reactions. As can be seen in Figure 10, no intercept was observed for **3a** in contrast to **3b** showing remarkable intercept. This difference may stem from the formation of the dead-end compound **4b** through the intramolecular reaction of **3b** (vide supra) in contrast with the lack of the formation of the corresponding N-oxide-coordinated complex from **3a**.

The quantum yields of the consumption of **3** were determined to be 0.0055 for **3a** and 0.019 for **3b**, respectively. These values are lower than those for **2a** and **2b** to afford **1a** (0.0057) and **1b** (0.028), respectively.[25] The reason for the lower quantum yields
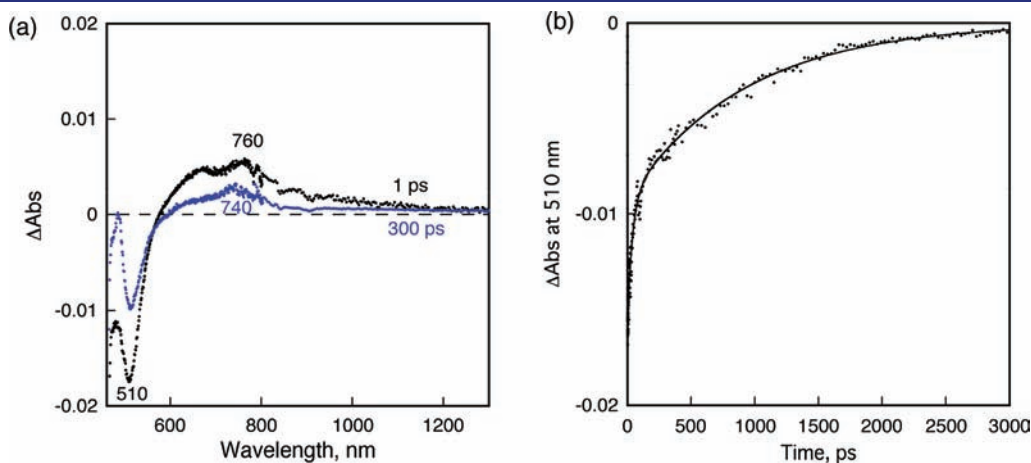

Figure 9. Femtosecond laser flash photolysis of **4b** in CH_3CN upon photoexcitation at 420 nm: (a) transient absorption spectra and (b) time course of absorbance at 510 nm.

may result from the intermolecular conversions of **3** to **5** and **6** in contrast with the intramolecular conversions of **2a** and **2b** to **1a** and **1b**, respectively.

In order to examine intermolecular oxygen atom transfer from the pendant pyridine *N*-oxide arm to another Ru(II) center, we conducted the reaction of **2** with excess amount of 2,6-dichloro-pyridine-*N*-oxide (Cl$_2$py-O) used as an external oxygen donor in CD$_3$CN under visible light irradiation. The ^{1}H NMR spectrum of the photoirradiated reaction mixture of **2b** and Cl$_2$py-O exhibited paramagnetically shifted peaks, which were consistent with those of **5b** formed by photoirradiation of **3b** as shown in Figure 11, as well as those of [Ru(O)(η^3-TPAH$^+$)(bpm)]$^{3+}$ formed by the reaction of **1b** with CAN (see Figure 6). These results also support the intermolecular oxo transfer between two **3b** molecules to generate **6b**.

Based on the observations described above, the photochemical reactions of **3b** are summarized in Scheme 3. The complex **3b** is excited by photoirradiation to perform structural change by releasing the CH$_3$CN ligand to afford the *N*-oxide-bound complex **4b** formed by the intramolecular reaction (pathway (w)). On the other hand, the intermolecular reaction (pathway (x)) affords **1b** and the Ru(IV)−oxo complex with the appended

N-oxide arm (**6b**). The complex **1b** undergoes photochromic structural change to give **2b** as previously reported.[25] The CH$_3$CN complex **2b** can react with the *N*-oxide moiety of **3b** to form the **5b** (pathway (z)). Alternatively, the complex **2b** can react with **6b** to generate **5b** via the intermolecular oxygen atom transfer (pathway (y)).

Substrate Oxygenation by 3a under Photoirradiation. We also examined oxygenation reactions of organic substrates (50 mM) with **3a** (5 mM) by photoirradiation at 420 nm under Ar at room temperature. The results were summarized in Table 1.

Cyclohexene was oxidized to afford cyclohexen-1-ol (14%) and cyclohexen-1-one (34%). With use of isolated [Ru^{IV}(O)(η^3-TPAH$^+$)(bpy)]$^{3+}$ synthesized by using CAN in CH$_3$CN at room temperature, cyclohexene was oxidized to be cyclohexen-1-ol (5%) and cyclohexen-1-one (46%).[26] This discrepancy may stem from the difference in the concentration of the oxidant: In light of the low quantum yield (0.0055) of the consumption of **3a** (vide supra), the concentrations of the reactive Ru(IV)−oxo complexes **5a** and **6a** formed by the photoreaction of **3a** should be inevitably lower than that of isolated [Ru^{IV}(O)(η^3-TPAH$^+$)-(bpy)]$^{3+}$. When cumene was used as a substrate, cumyl alcohol (24%) and acetophenone (6%) via β-scission of cumyl alkoxyl
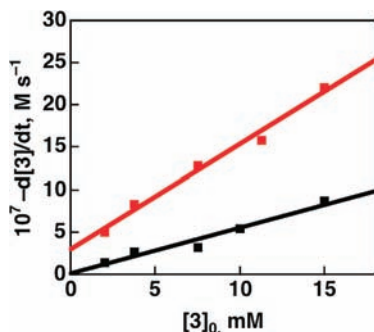
Figure 10. Dependence of decay rates of **3a** (black line) and **3b** (red line) in CD$_3$CN under photoirradiation on the initial concentrations of **3a** and **3b**, respectively.
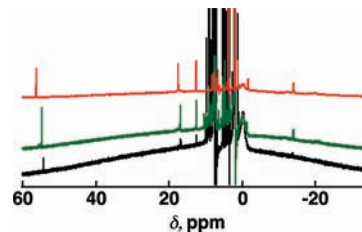
Figure 11. ^{1}H NMR spectrum of a solution containing [Ru^{IV}(O)(η^3-TPAH$^+$)(bpm)](PF$_6$)$_3$ (5 mM) formed by oxidation of **1b** by CAN in CD$_3$CN at room temperature (red trace), that of the reaction product by photoirradiation of **3b** (5 mM) in CD$_3$CN at room temperature (green line) and that by photoirradiation of the mixture of **2b** (5 mM) and 2,6-dichloropyridine *N*-oxide (100 mM) at 450 nm at room temperature (black line).

Scheme 3
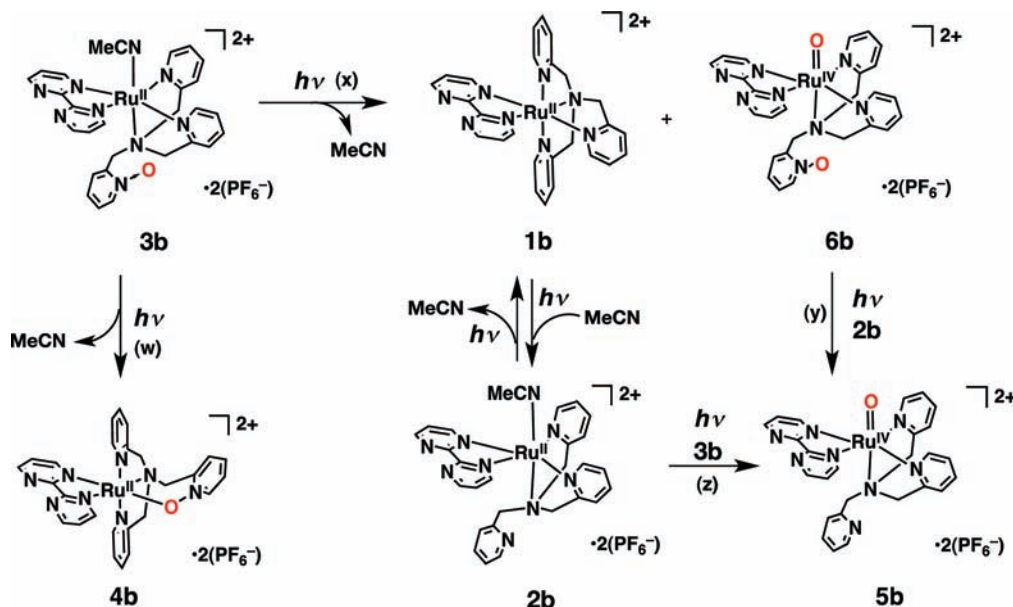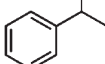
Table 1. Yields of Products in Oxidation of Various Substrates by 3a (5 mM) in Acetonitrile by Photoirradiation at 420 nm under Inert Atmosphere at Room Temperature

substrate	E_{ox} vs SCE (V)	BDE[a] (kcal/mol)	[sub] (mM)	product (yield %)	ox. eff.[d] (%)
(cyclohexene)	1.73^b	81.6	50	(ketone) $(34)^y$ (alcohol) $(14)^y$	82
(cumene)	2.14^c	84.8	50	(cumyl alcohol OH) $(34)^z$ (acetophenone O) $(6)^z$	46
(toluene)	2.20^c	88.5	500	(benzaldehyde O—H) $(6)^y$	18

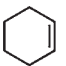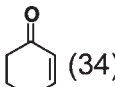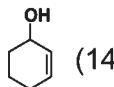[a] Taken from ref 29. [b] Taken from ref 30. [c] Taken from ref 31. Methods: y, by GC-MS in CH_3CN; z, by NMR and GC-MS in CD_3CN (y, 1,4-cyclohexadione as internal reference; z, methoxybenzene as internal reference). Products and their yields are based on **3a**. [d] Oxidation efficiency (%) = $[\{[\text{product(s)}]/(2 \times [\textbf{3a}])\} \times N(\text{oxidation equivalent})] \times 100$.

radical[32] were obtained by photoirradiation at 420 nm under Ar at room temperature. α-Methyl styrene, which can be formed by further oxidation of cumyl alcohol by $[\text{Ru}^{IV}(O)(\eta^3\text{-TPAH}^+)(\text{bpy})]^{3+}$,[26] was not obtained under photoirradiation of **3a**. This difference may be derived from the presence of proton in $[\text{Ru}^{IV}(O)(\eta^3\text{-TPAH}^+)(\text{bpy})]^{3+}$ to catalyze the dehydration of cumyl alcohol to give α-methyl styrene, while no proton is available for the reaction of **3a**. However, the ratio of [cumyl alcohol]/[acetophenone] (= 4) was similar to that observed in the reaction with use of $[\text{Ru}^{IV}(O)(\eta^3\text{-TPAH}^+)(\text{bpy})]^{3+}$.[26] When toluene was used as a substrate, benzaldehyde (6%) was obtained as the sole product. This result is consistent with that of isolated $[\text{Ru}^{IV}(O)(\eta^3\text{-TPAH}^+)(\text{bpy})]^{3+}$ used as an oxidant with respect to t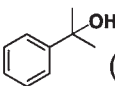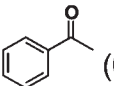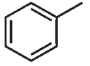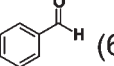he product.[26] The lower oxidation efficiency in the toluene oxygenation compared to that (23%) of the isolated $[\text{Ru}^{IV}(O)(\eta^3\text{-TPAH}^+)(\text{bpy})]^{3+}$ may result from the thermal self-decay of **5a** and **6a** by the heat of the light source.

In the oxygenation reaction of cyclohexene (50 mM) with **3a** (5 mM) under air, an unexpectedly large amount of cyclohexen-1-hydroperoxide (5.6 mM) was detected by ^{1}H NMR spectroscopy (Figure S8 in SI).[33] This product may come from the oxidation not by the Ru—oxo complex, but by singlet oxygen[34] because cyclohexene hydroperoxide is known to be formed by the reaction between cyclohexene and singlet oxygen derived from the photoirradiation of 9-phenylacridine in the presence of dioxygen.[35] Because it is well-known that the singlet oxygen can be produced by photosensitization with $[\text{Ru}^{II}(\text{bpy})_3]^{2+}$ under air,[36] the Ru(II)-bpy moiety of **3a** may also act as a photosensitizer to afford singlet oxygen by photoirradiation under aerobic atmosphere to give cyclohexen-1-hydroperoxide.

■ SUMMARY AND CONCLUSION

Ru(II)—diimine complexes having a η^1-CH_3CN ligand and a η^3-TPA ligand in a *facial* fashion with an uncoordinated pyridine arm, $[\text{Ru(TPA)(diimine)(CH}_3\text{CN})]^{2+}$, reacted with *m*CPBA to undergo oxygenation of the uncoordinated pyridine nitrogen. The Ru(II) complexes having uncoordinated pyridine-N-oxide arm exhibited photochemical transformation to afford an

N-oxide-chelated Ru(II) complex for the bpm complex and $[\text{Ru(TPA)(diimine)}]^{2+}$ with η^4-TPA, in addition to intermediate-spin ($S = 1$) Ru(IV)—oxo complexes in CH_3CN. The formation of the Ru(IV)—oxo complexes was revealed to proceed via photoinduced *intermolecular* oxygen atom transfer from the pyridine-N-oxide pendant to a Ru(II) center of another complex having CH_3CN as the leaving ligand. The Ru(IV)—oxo complex derived from $[\text{Ru}(\eta^3\text{-TPA-O})(\text{bpy})(CH_3CN)]^{2+}$ was demonstrated to oxygenate organic substrates. The results presented here have given the first clear evidence for the formation of high-valent Ru—oxo complexes by the reaction of pyridine-N-oxide with Ru(II) complexes via intermolecular pathway, even though the Ru(II) complex possesses a pyridine-N-oxide moiety. Together with the importance of pyridine-N-oxides as cleaner and safer terminal oxidants in organic synthesis than peroxides, the clarification of the reaction pathway of photoactivation of pyridine-N-oxides at the metal center to generate the reactive metal—oxo species provides valuable mechanistic insights into important oxidation processes.

■ EXPERIMENTAL SECTION

Materials. Acetonitrile in extra-pure grade was used without further purification. Diimine ligands were purchased from commercial sources and used without further purification. All other solvents were of special grade and were used as received from commercial sources without further purification. $\text{TPA}\cdot3\text{HClO}_4$,[37] $[\text{RuCl(TPA)}]_2(\text{ClO}_4)_2$,[38] $[\text{Ru(TPA)}(\text{bpy})](\text{PF}_6)_2$,[25] $[\text{Ru}(\eta^3\text{-TPA})(\text{bpy})(CH_3CN)](\text{PF}_6)_2$,[25a] $[\text{Ru(TPA)}(\text{bpm})](\text{PF}_6)_2$,[25a] $[\text{Ru}(\eta^3\text{-TPA})(\text{bpm})(CH_3CN)](\text{PF}_6)_2$[25a] were synthesized in the procedure reported previously. *m*-Chloroperbenzoic acid (*m*CPBA) was purified by the literature method.[39] Cyclohexene was purified by passage through a column of alumina to remove the BHT stabilizer.

Instrumentation. UV—vis spectra were collected on a Hewlett-Packard HP8453 photodiode array spectrophotometer. ^{1}H NMR spectra were recorded on JEOL JMN-AL-300 and Varian UNITY-600 NMR spectrometers at room temperature. Gas chromatographic analyses were performed on an Inertcap 5ms/sil column (GL Science, 30 m) and a mass spectrometer (Shimadzu QP 5000) as a detector. ESI-MS spectra were recorded on a Perkin-Elmer API-150 spectrometer. An Asahi Spectra MAX-301 was used for the light source.

[Ru(η^3-TPA-O)(bpy)(CH$_3$CN)](PF$_6$)$_2$ (3a). *m*CPBA (98 mg, 0.569 mmol) was added to a solution of [Ru(η^3-TPA)(bpy)(CH$_3$CN)]-(PF$_6$)$_2$ (100 mg, 0.114 mmol) in CH$_3$CN (100 mL). The mixture was heated to 50 °C for 24 h and evaporated to dryness to obtain a light orange powder. The powder was washed with diethyl ether and then dried *in vacuo* (85.1 mg, yield 83%). Anal. Calcd for C$_{30}$H$_{29}$ON$_7$-P$_2$F$_{12}$Ru: C, 40.28; H, 3.27; N, 10.96. Found: C, 40.42; H, 3.14; N, 10.87. ^{1}H NMR (CD$_3$CN): 8.92 (d, 2H, *J* = 6 Hz, bpy-*H*$_6$), 8.53 (d, 2H, *J* = 7 Hz, pyr-*H*$_6$ (equatorial)), 8.40 (d, 2H, *J* = 6 Hz, pyr-*H*$_3$(equatorial)), 8.14 (td, 2H, *J* = 8 and 2 Hz, pyr-*H*$_5$(equatorial)), 8.13 (dd, 1H, *J* = 7 and 1 Hz, pyr-*H*$_6$(free)), 7.79 (td, 2H, *J* = 8 and 2 Hz, bpy-*H*$_4$), 7.57 (ddd, 1H, *J* = 8 and 6 and 1 Hz, pyr-*H*$_4$(equatorial)), 7.43 (dd, 1H, *J* = 8 and 2 Hz, pyr-*H*$_3$(free)), 7.37 (ddd, 1H, *J* = 8 and 7 and 2 Hz, pyr-*H*$_5$(free)), 7.36 (dd, 2H, *J* = 8 and 6 Hz, bpy-*H*$_5$), 7.31 (d, 2H, *J* = 8 Hz, bpy-*H*$_3$), 7.30 (td, 1H, *J* = 8 and 1 Hz, pyr-*H*$_4$(free)), 4.92 and 4.11 (ABq, 4H, *J*$_{AB}$ = 17 Hz, *CH*$_2$(equatorial)), 3.48 (s, 2H, *CH*$_2$(free)), 2.29 (s, 3H, *CH*$_3$). ESI-MS (*m/z*): 750.1 ({M − (PF$_6$)}$^+$). Absorption maximum (λ_{max}, nm): 426. A single crystal of this compound was obtained by recrystallization from acetonitrile with vapor diffusion of diethyl ether.

[Ru(η^3-TPA-O)(bpm)(CH$_3$CN)](PF$_6$)$_2$ (3b). *m*CPBA (98 mg, 0.569 mmol) was added to a solution of [Ru(η^3-TPA)(bpm)(CH$_3$-CN)](PF$_6$)$_2$ (100 mg, 0.114 mmol) in CH$_3$CN (100 mL). The mixture was heated to 50 °C for 24 h and evaporated to dryness to obtain a light orange powder. The powder was washed with diethyl ether and then dried *in vacuo*. (83.2 mg Yield 81%. Anal. Calcd for C$_{28}$H$_{27}$ON$_9$-P$_2$F$_{12}$Ru: C, 37.43; H, 3.04; N, 14.06. Found: C, 37.51; H, 3.08; N, 14.14. ^{1}H NMR (CD$_3$CN): 9.20 (dd, 2H, *J* = 5 and 2 Hz, bpm-*H*$_6$), 8.91 (d, 2H, *J* = 6 Hz, pyr-*H*$_6$(equatorial)), 8.61 (dd, 2H, *J* = 4 and 2 Hz, bpm-*H*$_4$), 8.14 (d, 1H, *J* = 6 Hz, pyr-*H*$_6$(free)), 7.84 (td, 2H, *J* = 8 and 1 Hz, pyr-*H*$_4$(equatorial)), 7.70 (dd, 2H, *J* = 5 and 4 Hz, bpm-*H*$_5$), 7.45 (dd, 1H, *J* = 8 and 2 Hz, pyr-*H*$_3$(free)), 7.41 (t, 2H, *J* = 6 Hz, pyr-*H*$_5$(equatorial)), 7.39 (ddd, 2H, *J* = 8 and 6 and 2 Hz, pyr-*H*$_5$(free)), 7.35 (d, 2H, *J* = 8 Hz, pyr-*H*$_3$(equatorial)), 7.32 (td, 1H, *J* = 8 and 1 Hz, pyr-*H*$_4$(free)), 4.92 and 4.14 (ABq, 4H, *J*$_{AB}$ = 16 Hz, *CH*$_2$(equatorial)), 3.64 (s, 2H, *CH*$_2$(free)), 2.29 (s, 3H, *CH*$_3$). ESI-MS (*m/z*): 752.0 ({M − (PF$_6$)}$^+$). Absorption maximum (λ_{max}, nm): 449.

[(Ru-O-TPA)(bpm)](PF$_6$)$_2$ (4b). [Ru(η^3-TPA-O)(bpm)(CH$_3$CN)]-(PF$_6$)$_2$ (5 mg, 0.0057 mmol) was irradiated at 420 nm for 3 h in CH$_3$CN (0.6 mL). A dark brown single crystal of **4b** was obtained by recrystallization of the mixture from acetonitrile with vapor diffusion of diethyl ether. [Ru(TPA)(bpm)](PF$_6$)$_2$ (**1b**) will be obtained as a mixture when too much ether is added. Anal. Calcd for C$_{26}$H$_{24}$ON$_8$P$_2$F$_{12}$Ru: C, 36.50; H, 2.83; N, 13.10. Found: C, 36.64; H, 2.99; N, 12.84. ^{1}H NMR (CD$_3$CN): 10.38 (dd, 1H, *J* = 6 and 5 Hz, bpm-*N5,7-H*$_6$), 9.21 (dd, 1H, *J* = 5 and 2 Hz, bpm-*N5,7-H*$_4$), 9.14 (dd, 1H, *J* = 6 and 2 Hz, bpm-*N6,8-H*$_6$), 8.79 (dd, 1H, *J* = 5 and 2 Hz, bpm-*N6,8-H*$_4$), 8.61 (d, 1H, *J* = 7 Hz, pyr-*N3-H*$_6$), 8.01 (dd, 1H, *J* = 6 and 5 Hz, bpm-*N5,7-H*$_5$), 7.76 (dd, 1H, *J* = 8 and 2 Hz, pyr-*N3-H*$_3$), 7.74 (ddd, 1H, *J* = 8 and 7 and 1 Hz, pyr-*N4-H*$_5$), 7.64 (dd, 1H, *J* = 9 and 8 Hz, pyr-*N3-H*$_4$), 7.63 (dd, 1H, *J* = 7 and 1 Hz, pyr-*N4-H*$_3$), 7.59 (d, 1H, *J* = 8 Hz, pyr-*N4-H*$_6$), 7.53 (dd, 1H, *J* = 6 and 1 Hz, pyr-*N2-H*$_6$), 7.45 (dd, 1H, *J* = 6 and 5 Hz, bpm-*N6,8-H*$_5$), 7.37 (dd, 1H, *J* = 8 and 7 Hz, pyr-*N2-H*$_4$), 7.36 (ddd, 1H, *J* = 9 and 7 and 2 Hz, pyr-*N3-H*$_5$), 7.16 (t, 1H, *J* = 7 Hz, pyr-*N4-H*$_4$), 7.07 (d, 1H, *J* = 8 Hz, pyr-*N2-H*$_3$), 6.74 (dd, 1H, *J* = 7 and 6 Hz, pyr-*N2-H*$_5$), 5.34 and 5.09 (ABq, 2H, *J*$_{AB}$ = 18 Hz, *CH*$_2$), 5.28 and 5.20 (ABq, 2H, *J*$_{AB}$ = 16 Hz, *CH*$_2$(pyr-*N3* and *N4*)), 4.49 and 3.65 (ABq, 4H, *J*$_{AB}$ = 13 Hz, *CH*$_2$(pyr-*N2*)). Absorption maximum (λ_{max}, nm): 493. ESI-MS (*m/z*): 711.1 ({M − (PF$_6$)}$^+$). A single crystal of this compound was obtained by recrystallization from acetonitrile with vapor diffusion of diethyl ether.

Kinetic Analysis of the Reaction of 2a with *m*CPBA. *m*CPBA (2.9 mM, 5.8 mM, or 11.6 mM) was added to a CD$_3$CN solution of **2a** (1.15 mM). The reaction was performed in an oil bath kept at 323 K. ^{1}H NMR spectra were recorded to monitor the reaction for one-hour or

five-hours intervals by observing time course of the signals due to the axial methylene protons of **2a** and **3a**. The time-course of [**3a**]/{[**2a**] + [**3a**]} was plotted and curve-fitting of the data was made by using the following equation:

$$F(t) = A + B\exp(-k_{obs}t)$$

where *A* and *B* are coefficients, *t* is the reaction time (s), and k_{obs} is the pseudo-first-order rate constant, respectively.

Resonance Raman Spectroscopy on [Ru(O)(η^3-TPAH$^+$)-(bpm)]$^{3+}$. Samples were prepared by the following procedures. For [Ru(^{16}O)(η^3-TPAH$^+$)(bpm)]$^{3+}$, CAN (8.8 mg, 16.0 μmol) was added to 1 mL of a H$_2$^{16}O solution of [Ru(TPA)(bpm)](PF$_6$)$_2$ (1.7 mg, 2.0 μmol) and stirred for 2 min. For [Ru(^{18}O)(η^3-TPAH$^+$)(bpm)]$^{3+}$, CAN (1.8 mg, 3.2 μmol) was added to 200 μL of a H$_2$^{18}O solution of [Ru(TPA)(bpm)](PF$_6$)$_2$ (0.3 mg, 0.4 μmol) and stirred for 2 min. Resonance Raman scattering was made by excitation at 363.8 nm with an Ar$^+$ laser (Spectra Physics, 2080-25/2580C), dispersed by a single polychromator (Ritsu Oyo Kogaku, MC-100DG) and detected by a liquid-nitrogen-cooled CCD detector (Roper Scientific, LNCCD-1100-PB). The resonance Raman measurements were carried out at 22 °C using a spinning cell (outer diameter = 3 mm, wall thickness = 1 mm) at 90° scattering geometry.

Photochemical Reactions. Photoirradiation of the samples was performed by using the light source of an Asahi Spectra MAX-301 at monochromated wavelengths (420 ± 5 or 450 ± 5 nm) in CD$_3$CN at room temperature. The reaction was done in an NMR tube or a 10 mm quartz cell to monitor the progress of the reaction by NMR and absorption spectroscopy, respectively. All experiments were performed under an inert atmosphere using standard techniques unless otherwise noted.

Photoreactions of 3a, 3b, and 4b in the Absence of Substrate. The complexes (3.0 μmol) were dissolved in CD$_3$CN (600 μL) and irradiated by using the light source of an Asahi Spectra MAX-301 at monochromated wavelengths ([Ru(η^3-TPA-O)(bpy)(CH$_3$CN)](PF$_6$)$_2$ (**3a**), 420 nm; [Ru(η^3-TPA-O)(bpm)(CH$_3$CN)](PF$_6$)$_2$ (**3b**), 450 nm; [(Ru-O-TPA)(bpm)](PF$_6$)$_2$ (**4b**), 450 nm). The reactions were monitored by ^{1}H NMR measurements every hour.

Determination of the Initial Decay Rate of Photoreactions of 3a and 3b in the Absence of Substrate. The complexes (3.3, 6.2, 12, 16, 25 mM for **3a**; 3.3, 6.2, 12, 19, 25 mM for **3b**) were dissolved in CD$_3$CN (600 μL) and photoirradiated by using an Asahi Spectra MAX-301 at monochromated wavelengths: For ([Ru(η^3-TPA-O)-(bpy)(CH$_3$CN)](PF$_6$)$_2$ (**3a**), 420 nm; for [Ru(η^3-TPA-O)(bpm)-(CH$_3$CN)](PF$_6$)$_2$ (**3b**), 450 nm). The reactions were monitored by ^{1}H NMR measurements every 20 min. The decay rates were determined using the following equation:

$$\text{decay rate} = -d[\mathbf{3}]/dt = ([\mathbf{3}]_0 - [\mathbf{3}]_t)/t$$

where [**3**]$_t$ is concentration of **3** at certain time *t* (s), [**3**]$_0$ is a initial concentration of **3** and *t* (s) is reaction time, which was 6000 s (100 min) for **3a** and 4800 s (80 min) for **3b**. Therefore, the decrease in the concentration of **3** for 100 min for **3a** and 80 min for **3b** were divided by 6000 and 4800, respectively.

Photoirradiation in the Presence of Substrate. In a 10 mm quartz cell, a complex (4.5 μmol) and a substrate (45−450 μmol) were added in CD$_3$CN (900 μL) and photoirradiated under Ar atmosphere by using the light source of an Asahi Spectra MAX-301 at monochromated wavelengths ([Ru(η^3-TPA-O)(bpy)(CH$_3$CN)](PF$_6$)$_2$ (**3a**), 420 nm; [(Ru-O-TPA)(bpm)](PF$_6$)$_2$ (**4b**), 450 nm). ^{1}H NMR and GC-MS measurements were made after 30 h.

X-ray Crystallography. The crystals of **2a**, **3a**, and **4b** were mounted on a glass capillary with epoxy resin. All measurements were performed on a Rigaku Mercury CCD diffractometer at −150 °C with a graphite-monochromated Mo Kα radiation (λ = 0.71073 Å). The data

17908

dx.doi.org/10.1021/ja207572z |*J. Am. Chem. Soc.* 2011, 133, 17901–17911

Table 2. X-ray Crystallographic Data for $[\mathrm{Ru}(\eta^3\text{-TPA})(\mathrm{bpy})(\mathrm{CH_3CN})](\mathrm{PF_6})_2$ (2a), $[\mathrm{Ru}(\eta^3\text{-TPA-O})(\mathrm{bpy})(\mathrm{CH_3CN})](\mathrm{PF_6})_2$ (3a), and $[(\mathrm{Ru\text{-}O\text{-}TPA})(\mathrm{bpm})](\mathrm{PF_6})_2$ (4b)

	2a	3a	4b
formula	$C_{30}H_{29}F_{12}N_7P_2Ru$	$C_{30}H_{29}N_7OP_2F_{12}Ru$	$C_{26}H_{24}N_8OP_2F_{12}Ru$
fw	878.60	894.61	855.53
crystal system	monoclinic	monoclinic	triclinic
space group	$P2_1/n$	$P2_1/n$	$P\bar{1}$
T, K	123	123	123
a, Å	19.25(8)	19.373(3)	11.343(2)
b, Å	9.01(4)	8.841(1)	12.621(3)
c, Å	21.80(9)	21.969(3)	12.733(3)
α, deg			72.79(6)
β, deg	115.04(2)	114.9229(4)	77.87(6)
γ, deg			74.91(6)
V, Å³	3427(25)	3412.6(8)	1663.7(6)
Z	4	4	2
no. of reflections	26126	25656	13225
no. of observations	7740	7574	7303
no. of parameters	470	479	479
$R1^a$ ($I > 2.0\sigma(I)$)	0.101	0.053	0.055
$wR2^b$ (all data)	0.238	0.138	0.147
GOF	1.22	1.11	1.05

$^a R1 = \|F_o| - |F_c\|/\Sigma |F_o|.$ $^b wR2 = [\Sigma(w(F_o^2 - F_c^2)^2)/\Sigma w(F_o^2)^2]^{1/2}.$

were collected up to $2\theta = 55.0°$. The structure was solved by direct methods and expanded using Fourier techniques. All non-hydrogen atoms were refined anisotropically. Refinement was carried out with full-matrix least-squares on F with scattering factors[40] and including anomalous dispersion effects.[41] All calculations were performed using the Crystal Structure crystallographic software package,[42] and structure refinements were made by using SHELX-97.[43] Crystallographic data are summarized in Table 2.

Quantum Yield Determination. Quantum yields of the reactions were determined by a standard method using an actinometer (potassium ferrioxalate) in CD_3CN at room temperature with photoirradiation at 420 nm. Absorbance of the complex and that of the actinometer were uniformed at 420 nm to determine the quantum yields. The reactions were monitored at the decay of the peak of **3** (7.5 mM) in NMR spectra and the data at the initial stage, where the time-course of the spectral change was linear, were used to determine the quantum yields.

Femtosecond Laser Flash Photolysis of 4b. A CH_3CN solution of **4b** (0.083 mM) was prepared for laser flash photolysis. Femtosecond transient absorption spectroscopy experiments were conducted using an ultrafast source: Integra-C (Quantronix Corp.), an optical parametric amplifier: TOPAS (Light Conversion Ltd.) and a commercially available optical detection system: Helios provided by Ultrafast Systems LLC. The source for the pump and probe pulses were derived from the fundamental output of Integra-C (780 nm, 2 mJ/pulse and fwhm = 130 fs) at a repetition rate of 1 kHz. 75% of the fundamental output of the laser was introduced into TOPAS which has optical frequency mixers resulting in tunable range from 285 to 1660 nm, while the rest of the output was used for white light generation. Prior to generating the probe continuum, a variable neutral density filter was inserted in the path in order to generate stable continuum, then the laser pulse was fed to a delay line that provides an experimental time window of 3.2 ns with a maximum step resolution of 7 fs. Excitation wavelength at 420 nm of TOPAS output, which is fourth harmonic of signal or idler pulses, was chosen as the pump beam. As this TOPAS output consists of not only desirable wavelength

but also unnecessary wavelengths, the latter was deviated using a wedge prism with wedge angle of 18 degree. The desirable beam was irradiated at the sample cell with a spot size of 1 mm diameter where it was merged with the white probe pulse in a close angle (<10 degree). The probe beam after passing through the 2 mm sample cell was focused on a fiber optic cable, which was connected to a CCD spectrograph for recording the time-resolved spectra (470–1600 nm). Typically, 3000 excitation pulses were averaged for 3 s to obtain the transient spectrum at a set delay time. Kinetic traces at appropriate wavelengths were assembled from the time-resolved spectral data. All measurements were conducted at room temperature, 295 K.

■ ASSOCIATED CONTENT

ⓢ **Supporting Information.** Figures S1–S8 and crystallographic data for **2a**, **3a**, and **4b** in CIF format. This material is available free of charge via the Internet at http://pubs.acs.org.

■ AUTHOR INFORMATION

Corresponding Author
kojima@chem.tsukuba.ac.jp; fukuzumi@chem.eng.osaka-u.ac.jp

■ ACKNOWLEDGMENT

17909

dx.doi.org/10.1021/ja207572z |*J. Am. Chem. Soc.* 2011, 133, 17901–17911

■ REFERENCES

(1) (a) Sheldon, R. A.; Kochi, J. K. *Metal-Catalyzed Oxidations of Organic Compounds*; Academic Press: New York, 1981. (b) *Activation and Functionalization of Alaknes*; Hill, C. L., Ed.: Wiley: New York, 1989. (c) *The Activation of Dioxygen and Homogeneous Catalytic Oxidation*; Barton, D. H. R., Martell, A. E., Sawyer, D. T., Eds.; Plenum: New York, 1993. (d) Shilov, A. E.; Shul'pin, G. B. *Chem. Rev.* **1997**, *97*, 2879–2932. (e) *Biomimetic Oxidations Catalyzed by Transition Metal Complexes*; Meunier, B., Ed.; Imperial College Press: London, 2000.

(2) (a) Gunay, A.; Theopold, K. H. *Chem. Rev.* **2010**, *110*, 1060–1081. (b) Kolb, H. C.; VanNieuwenhze, M. S.; Sharpless, K. B. *Chem. Rev.* **1994**, *94*, 2483–2547.

(3) (a) Meunier, B.; de Visser, S. P.; Shaik, S. *Chem. Rev.* **2004**, *104*, 3947–3980. (b) Groves, J. T. *Proc. Natl. Acad. Sci. U.S.A.* **2004**, *100*, 3569–3574.

(4) (a) Sato, K.; Aoki, M.; Noyori, R. *Science* **1998**, *281*, 1646–1647. (b) Chen, M. S.; White, M. C. *Science* **2007**, *318*, 783–787. (c) Lane, B. S.; Burgess, K. *Chem. Rev.* **2003**, *103*, 2457–2473. (d) Kamata, K.; Yonehara, K.; Sumida, Y.; Yamaguchi, K.; Hikichi, S.; Mizuno, N. *Science* **2003**, *300*, 964–966. (e) de Boer, J. W.; Brinksma, J.; Browne, W. R.; Meetsma, A.; Alsters, P. L.; Hage, R.; Feringa, B. L. *J. Am. Chem. Soc.* **2005**, *127*, 7990–7991.

(5) (a) Que, L., Jr.; Tolman, W. B. *Angew. Chem., Int. Ed.* **2002**, *41*, 1114–1137. (b) Rhode, J.-U.; In, J.-H.; Lim, M. H.; Brennessel, W. W.; Bukowski, M. R.; Stubna, A.; Münck, E.; Nam, W.; Que, L., Jr. *Science* **2003**, *299*, 1037–1039. (c) Nam, W. *Acc. Chem. Res.* **2007**, *40*, 522–531. (d) Que, L., Jr. *Acc. Chem. Res.* **2007**, *40*, 493–500. (e) Fiedler, A. T.; Que, L. *Inorg. Chem.* **2009**, *48*, 11038–11047. (f) Hirao, H.; Chen, H.; Carvajal, M. A.; Wang, Y.; Shaik, S. *J. Am. Chem. Soc.* **2008**, *130*, 3319–3327. (g) Takahashi, A.; Kurahashi, T.; Fujii, H. *Inorg. Chem.* **2007**, *46*, 6227. (h) Yip, W.-P.; Yu, W.-Y.; Zhu, N.; Che, C.-M. *J. Am. Chem. Soc.* **2005**, *127*, 14239–14249.

(6) (a) Groves, J. T.; Nemo, T. E. *J. Am. Chem. Soc.* **1983**, *105*, 6243–6248. (b) Fujii, H. *J. Am. Chem. Soc.* **1993**, *115*, 4641–4648. (c) Auclair, K.; Hu, Z.; Little, D. M.; Ortiz de Montellano, P. R.; Groves, J. T. *J. Am. Chem. Soc.* **2002**, *124*, 6020–6027.

(7) For Fe: (a) Kaizer, J.; Klinker, E. J.; Oh, A. Y.; Rohde, J.-U.; Song, W. J.; Stubna, A.; Kim, J.; Münck, E.; Nam, W.; Que, L., Jr. *J. Am. Chem. Soc.* **2004**, *126*, 472–473. (b) Brazeau, B. J.; Austin, R. N.; Tarr, C.; Groves, J. T.; Lipscomb, J. D. *J. Am. Chem. Soc.* **2001**, *123*, 11831–11837. (c) Oldenburg, P. D.; Feng, Y.; Pryjomska-Ray, I.; Ness, D.; Que, L., Jr. *J. Am. Chem. Soc.* **2010**, *132*, 17713–17723.

(8) For Ru: (a) Thompson, M. S.; Meyer, T. J. *J. Am. Chem. Soc.* **1982**, *104*, 4106–4115. (b) Thompson, M. S.; Meyer, T. J. *J. Am. Chem. Soc.* **1982**, *104*, 5070–5076. (c) Stultz, L. K.; Huynh, H. V.; Binstead, R. A.; Curry, M.; Meyer, T. J. *J. Am. Chem. Soc.* **2000**, *122*, 5984–5996. (d) Bryant, J. R.; Mayer, J. M. *J. Am. Chem. Soc.* **2003**, *125*, 10351–10361. (e) Bryant, J. R.; Matsuo, T.; Mayer, J. M. *Inorg. Chem.* **2004**, *43*, 1587–1592.

(9) For other metals: (a) Gardner, K. A.; Mayer, J. M. *Science* **1995**, *269*, 1849–1851. (b) Fukuzumi, S.; Kishi, T.; Kotani, H.; Lee, Y.-M.; Nam, W. *Nat. Chem.* **2011**, *3*, 38–41.

(10) (a) Groves, J. T.; Watanabe, Y. *J. Am. Chem. Soc.* **1986**, *108*, 7834–7836. (b) Groves, J. T.; Watanabe, Y. *J. Am. Chem. Soc.* **1988**, *110*, 8443–8452. (c) Yamaguchi, K.; Watanabe, Y.; Morishima, I. *J. Am. Chem. Soc.* **1993**, *115*, 4058–4065.

(11) (a) Nam, W.; Han, H. J.; Oh, S.-Y.; Lee, Y. J.; Choi, M.-H.; Han, S.-Y.; Kim, C.; Woo, S. K.; Shin, W. *J. Am. Chem. Soc.* **2000**, *122*, 8677–8684. (b) Nam, W.; Lim, M. H.; Moon, S. K.; Kim, C. *J. Am. Chem. Soc.* **2000**, *122*, 10805–10809.

(12) Heme enzymes: (a) Dawson, J. H.; Sono, M. *Chem. Rev.* **1987**, *87*, 1255–1276. (b) Sono, M.; Roach, M. P.; Coulter, E. D.; Dawson, J. H. *Chem. Rev.* **1996**, *96*, 2841–2888. (c) Schlichting, I.; Berendzen, J.; Chu, K.; Stock, A. M.; Maves, S. A.; Benson, D. E.; Sweet, R. M.; Ringe, D.; Petsko, G. A.; Sligar, S. G. *Science* **2000**, *287*, 1615–1622. (d) Denisov, I. D.; Makris, T. M.; Sliger, S. G.; Schlichting, I. *Chem. Rev.* **2005**, *105*, 2253–2277. (e) Ortiz de Montellano, P. R. *Chem. Rev.* **2010**, *110*, 932–948.

(13) Non-heme enzymes: (a) Wallar, B. J.; Lipscomb, J. D. *Chem. Rev.* **1996**, *96*, 2625–2658. (b) Lippard, S. J. *J. Chem. Soc., Dalton Trans.* **1997**, 3925. (c) Costas, M.; Mehn, M. P.; Jensen, M. P.; Que, L., Jr. *Chem. Rev.* **2004**, *104*, 939–986. (d) Abu-Omar, M. M.; Loaiza, A.; Hontzeas, N. *Chem. Rev.* **2005**, *105*, 2227–2252.

(14) (a) Punniyamurthy, T.; Velusamy, S.; Iqbal, J. *Chem. Rev.* **2005**, *105*, 2329–2363. (b) Jiang, B.; Feng, Y.; Ison, E. A. *J. Am. Chem. Soc.* **2008**, *130*, 14462–14464. (c) Leising, R. A.; Takeuchi, K. J. *Inorg. Chem.* **1987**, *26*, 4391–4393. (d) Shimizu, H.; Onitsuka, S.; Egani, H.; Katsuki, T. *J. Am. Chem. Soc.* **2005**, *127*, 5396–5413. (e) Mirica, L. M.; Vance, M.; Rudd, D. J.; Hedman, B.; Hodgson, K. O.; Solomon, E. I.; Stack, T. D. P. *Science* **2005**, *308*, 1890–1892. (f) Goldstein, A. S.; Beer, R. H.; Drago, R. S. *J. Am. Chem. Soc.* **1994**, *116*, 2424–2429. (g) Sawada, Y.; Matsumoto, K.; Katsuki, T. *Angew. Chem., Int. Ed.* **2007**, *46*, 4559–4561. (h) Jain, S. L.; Sain, B. *Chem. Commun.* **2002**, 1040–1041. (i) Kojima, T.; Matsuda, Y. *Chem. Lett.* **1999**, 81–82.

(15) Horseradish peroxidase: (a) Berglund, J.; Pascher, T.; Winkler, J. R.; Gray, H. B. *J. Am. Chem. Soc.* **1997**, *119*, 2464–2469. (b) Rodríguez-López, J. N.; Lowe, D. J.; Hernández-Ruiz, J.; Hinter, A. N. P.; García-Cánovas, F.; Thorneley, R. N. F. *J. Am. Chem. Soc.* **2001**, *123*, 11838–11847. (c) Berglund, G. I.; Carlsson, G. H.; Smith, A. T.; Szöke, H.; Henriksen, A.; Hadju, J. *Nature* **2002**, *417*, 463–468.

(16) H_2O_2: (a) Sawada, Y.; Matsumoto, K.; Katsuki, T. *Angew. Chem., Int. Ed.* **2007**, *46*, 4559–4561. (b) Fujita, M.; Costas, M.; Que, L., Jr. *J. Am. Chem. Soc.* **2003**, *125*, 9912–9913.

(17) Alkyl hydroperoxides: (a) Leising, R. A.; Kim, J.; Pérez, M.; Que, L., Jr. *J. Am. Chem. Soc.* **1993**, *115*, 9524–9530. (b) Kojima, T.; Leising, R. A.; Yan, S.; Que, L., Jr. *J. Am. Chem. Soc.* **1993**, *115*, 11328–11335. (c) Kim, J.; Harrison, R. G.; Kim, C.; Que, L., Jr. *J. Am. Chem. Soc.* **1996**, *118*, 4373–4379. (d) Jensen, M. P.; Costas, M.; Ho, R. Y. N.; Kaizer, J.; i Payeras, A. M.; Münck, E.; Que, L., Jr.; Rhode, J.-U.; Stubna, A. *J. Am. Chem. Soc.* **2005**, *127*, 10512–10525. (e) Kojima, T.; Matsuo, H.; Matsuda, Y. *Inorg. Chim. Acta* **2000**, *300–302*, 661–667. (f) Nguyen, C.; Guajardo, R. J.; Mascarak, P. K. *Inorg. Chem.* **1996**, *35*, 6273–6281. (g) Yl, C. S.; Kwon, K.-H.; Lee, D. W. *Org. Lett.* **2009**, *7*, 1567–1569.

(18) Peracids: (a) Kojima, T. *Chem. Lett.* **1996**, 121–122. (b) Lee, K. A.; Nam, W. *J. Am. Chem. Soc.* **1997**, *119*, 1916–1922. (c) Komiya, N.; Noji, S.; Murahashi, S. *Chem. Commun.* **2001**, 65–66. (d) Franke, A.; Wolak, M.; van Eldik, R. *Chem.—Eur. J.* **2009**, *15*, 10182–10198. (e) Palucki, M.; Pospisil, P. J.; Zhang, W.; Jacobsen, E. N. *J. Am. Chem. Soc.* **1994**, *116*, 9333–9334. (f) Kang, M.-J.; Song, W. J.; Han, A.-R.; Choi, Y. S.; Jang, H.-G.; Nam, W. *J. Org. Chem.* **2007**, *72*, 6301–6304. (g) Li, F.; Wang, M.; Ma, C.; Gao, A.; Chen, H.; Sun, L. *Dalton Trans.* **2006**, 2427–2434. (h) Kojima, T.; Hayashi, K.; Iizuka, S.; Tani, F.; Naruta, Y.; Kawano, M.; Ohashi, Y.; Hirai, Y.; Ohkubo, K.; Matsuda, Y.; Fukuzumi, S. *Chem.—Eur. J.* **2007**, *13*, 8212–8222.

(19) Iodosylarenes: (a) Nam, W.; Jin, S. W.; Lim, M. H.; Ryu, J. Y.; Kim, C. *Inorg. Chem.* **2002**, *41*, 3647–3652. (b) Reginato, G.; Di Bari, L.; Salvadori, P.; Guilard, R. *Eur. J. Org. Chem.* **2000**, 1165–1171. (c) Battioni, P.; Cardin, E.; Louloudi, M.; Schollhorn, B.; Spyroulias, G. A.; Mansuy, D.; Traylor, T. G. *Chem. Commun.* **1996**, 2037–2038. (d) Okumura, T.; Morishima, Y.; Shiozaki, H.; Yagyu, T.; Funahashi, Y.; Ozawa, T.; Jitsukawa, K.; Masuda, H. *Bull. Chem. Soc. Jpn.* **2007**, *80*, 507–517. (e) Nishiyama, H.; Shimada, T.; Itoh, H.; Sugiyama, H.; Motoyama, Y. *Chem. Commun.* **1997**, 1863–1864.

(20) PCET: (a) Moyer, B. A.; Thompson, M. S.; Meyer, T. J. *J. Am. Chem. Soc.* **1980**, *102*, 2310–2312. (b) Moyer, B. A.; Meyer, T. J. *Inorg. Chem.* **1981**, *20*, 436–444. (c) Che, C.-M.; Yam, V. W.-W.; Mak, T. C. W. *J. Am. Chem. Soc.* **1990**, *112*, 2284–2291. (d) Szczepura, L. F.; Maricich, S. M.; See, R. F.; Churchill, M. R.; Takeuchi, K. J. *Inorg. Chem.* **1995**, *34*, 4198–4205. (e) Che, C.-M.; Cheng, K.-W.; Chan, M. C. W.; Lau, T.-C.; Mak, C.-K. *J. Org. Chem.* **2000**, *65*, 7996–8000. (f) Meyer, T. J.; Huynh, M. H. V. *Inorg. Chem.* **2003**, *42*, 8140–8160. (g) Dhuri, S. N.; Seo, M. S.; Lee, Y.-M.; Hirao, H.; Wang, Y.; Nam, W.; Shaik, S. *Angew. Chem., Int. Ed.* **2008**, *47*, 3356–3359. (h) Hirai, Y.; Kojima, T.; Mizutani, Y.; Shiota, Y.; Yoshizawa, K.; Fukuzumi, S. *Angew. Chem., Int. Ed.* **2008**, *47*, 5772–5776. (i) Lee, Y.-M.; Dhuri, S. N.; Sawant, S. C.; Cho, J.;

17910

dx.doi.org/10.1021/ja207572z |*J. Am. Chem. Soc.* 2011, 133, 17901–17911

Kubo, M.; Ogura, T.; Fukuzumi, S. *Angew. Chem., Int. Ed.* **2009**, *48*, 1803–1806. (j) Bozoglian, F.; Romain, S.; Erten, M. Z.; Todorova, T. K.; Sens, C.; Mola, J.; Rodoríguez, M.; Romero, I.; Benet-Buchholz, J.; Fontrodona, X.; Cramer, C. J.; Gagliardi, L.; Llobet, A. *J. Am. Chem. Soc.* **2009**, *131*, 15176–15187. (k) Sartorel, A.; Miró, P.; Salvadori, E.; Romain, S.; Carrano, M.; Scorrano, G.; Valentin, M. D.; Llobet, A.; Bonchio, M. *J. Am. Chem. Soc.* **2009**, *131*, 16951–16053. (l) Kojima, T.; Hirai, Y.; Ikemura, K.; Ogura, T.; Shiota, Y.; Yoshizawa, K.; Fukuzumi, S. *Angew. Chem., Int. Ed.* **2010**, *49*, 8449–8453. (m) Sawant, S. C.; Wu, X.; Cho, J.; Cho, K.-B.; Kim, S. H.; Seo, M. S.; Lee, Y.-M.; Kubo, M.; Ogura, T.; Shaik, S.; Nam, W. *Angew. Chem., Int. Ed.* **2010**, *49*, 8190–8194.

(21) (a) Suslick, K. S.; Acholla, F. V.; Cook, B. R. *J. Am. Chem. Soc.* **1987**, *109*, 2818–2819. (b) Zhang, R.; Newcomb, M. *J. Am. Chem. Soc.* **2003**, *125*, 12418–12419. (c) Zhang, R.; Horner, J. H.; Newcomb, M. *J. Am. Chem. Soc.* **2005**, *127*, 6573–6582. (d) Harischandra, D. N.; Zhang, R.; Newcomb, M. *J. Am. Chem. Soc.* **2005**, *127*, 13776–13777. (e) Pan, Z.; Sheng, X.; Horner, J. H.; Newcomb, M. *J. Am. Chem. Soc.* **2009**, *131*, 2621–2628. (f) Harischandra, D. N.; Lowery, G.; Zhang, R.; Newcomb, M. *Org. Lett.* **2009**, *11*, 2089–2092.

(22) (a) Higuchi, T.; Ohtake, H.; Hirobe, M. *Tetrahedron Lett.* **1989**, *30*, 6545–6548. (b) Ohtake, H.; Higuchi, T.; Hirobe, M. *J. Am. Chem. Soc.* **1992**, *114*, 10660–10662. (c) Higuchi, T.; Satake, C.; Hirobe, M. *J. Am. Chem. Soc.* **1995**, *117*, 8879–8880. (d) Higuchi, T.; Hirobe, M. *J. Mol. Catal., A: Chem.* **1996**, *113*, 403–422. (e) Gross, Z.; Ini, S. *Inorg. Chem.* **1999**, *38*, 1446–1449. (f) Yamaguchi, M.; Kumano, T.; Masui, D.; Yamagishi, T. *Chem. Commun.* **2004**, 798–799. (g) Yamaguchi, M.; Tomizawa, M.; Takagaki, K.; Shimo, M.; Masui, D.; Yamagishi, T. *Catal. Today* **2006**, *117*, 206–209.

(23) (a) Zhang, R.; Yu, W.-Y.; Wong, K.-Y.; Che, C.-M. *J. Org. Chem.* **2001**, *66*, 8145–8153. (b) Zhang, J.-L.; Che, C.-M. *Chem.—Eur. J.* **2005**, *11*, 3899–3914. (c) Ito, R.; Umezawa, N.; Higuchi, T. *J. Am. Chem. Soc.* **2005**, *127*, 834–835. (d) Fackler, P.; Berthold, C.; Voss, F.; Bach, T. *J. Am. Chem. Soc.* **2010**, *132*, 15911–15913.

(24) Donohoe, T. J.; Wheelhouse, K. M. P.; Lindsay-Scott, P. J.; Glossop, P. A.; Nash, I. A.; Parkers, J. S. *Angew. Chem., Int. Ed.* **2008**, *47*, 2872–2875.

(25) (a) Kojima, T.; Morimoto, T.; Sakamoto, T.; Miyazaki, S.; Fukuzumi, S. *Chem.—Eur. J.* **2008**, *14*, 8904–8915. (b) Kojima, T.; Sakamoto, T.; Matsuda, Y. *Inorg. Chem.* **2004**, *43*, 2243–2245.

(26) Kojima, T.; Nakayama, K.; Ikemura, K.; Ogura, T.; Fukuzumi, S. *J. Am. Chem. Soc.* **2011**, *133*, 11692–11700.

(27) (a) Hirai, Y.; Kojima, T.; Mizutani, Y.; Shiota, Y.; Yoshizawa, K.; Fukuzumi, S. *Angew. Chem., Int. Ed.* **2008**, *47*, 5772–5776. (b) See also ref 20l.

(28) (a) Sharma, R.; Karmaker, A.; Baruah, J. B. *Inorg. Chim. Acta* **2008**, *361*, 2081–2086. (b) Deiters, E.; Bulach, V.; Hosseoni, M. W. *Dalton Trans.* **2007**, 4126–4131. (c) Nienkenper, K.; Kotov, V. V.; Kehr, G.; Erker, G.; Fröhlich, R. *Eur. J. Inorg. Chem.* **2006**, 366–379. (d) He, Z.; Wang, Z.-M.; Gao, S.; Yan, C.-H. *Inorg. Chem.* **2006**, *45*, 6694–6705. (e) Blake, A. B.; Sinn, E.; Yavari, A.; Moubaraki, B.; Murray, K. S. *Inorg. Chim. Acta* **1995**, *229*, 281–290. (f) Gembicky, A.; Baran, P.; Boca, R.; Fuess, H.; Svoboda, I.; Valco, M. *Inorg. Chim. Acta* **2000**, *303*, 75–82.

(29) Luo, Y.-R. *Handbook of Bond Dissociation Energies in Organic Compounds*; CRC Press: 2003.

(30) Siu, T.; Picard, C. J.; Yudin, A. K. *J. Org. Chem.* **2005**, *70*, 932–937.

(31) Fukuzumi, S.; Ohkubo, K.; Suenobu, T.; Kato, K.; Fujitsuka, M.; Ito, O. *J. Am. Chem. Soc.* **2001**, *123*, 8459–8467.

(32) Avila, D. A.; Brown, C. E.; Ingold, K. U.; Lusztyk, J. *J. Am. Chem. Soc.* **1993**, *115*, 466–470.

(33) Dang, H.-S.; Davies, A. G. *J. Chem. Soc., Perkin Trans. 2.* **1991**, 2011–2020.

(34) Xue, X.; Xu, Y. *J. Mol. Catal. A: Chem.* **2007**, *276*, 80.

(35) (a) Darmanyan, A. P.; Gregory, D. D.; Guo, Y.; Jenks, W. S.; Burel, L.; Eloy, D.; Jardon, P. *J. Am. Chem. Soc.* **1998**, *120*, 396–403. (b) Kristiansen, M.; Scurlock, R. D.; Iu, K. K.; Ogilby, P. R. *J. Phys. Chem.* **1991**, *95*, 5190–5197.

(36) (a) Zhang, X.; Rodgers, M. A. J. *J. Phys. Chem.* **1995**, *99*, 12797–12803. (b) Mulazzani, Q. G.; Ciano, M.; D'Angelantonio, M.; Venturi, M.; Rodgers, M. A. J. *J. Am. Chem. Soc.* **1988**, *110*, 2451–2457.

(37) (a) Anderegg, G; Wenk, F. *Helv. Chim. Acta* **1967**, *50*, 2330–2332. (b) Gafford, B. G.; Holewerda, R. A. *Inorg. Chem.* **1989**, *28*, 60–66.

(38) Kojima, T.; Amano, T.; Ishii, Y.; Ohba, M.; Okaue, Y.; Matsuda, Y. *Inorg. Chem.* **1998**, *37*, 4076–4085.

(39) Armarego, W. L. F.; Chai, C. L. L. *Purification of Laboratory Chemicals*, 6th ed.; Elsevier: Oxford, UK; 2009:

(40) Creagh, D. C.; McAuley, W. J. In *International Tables for Crystallography*; Wilson, A. J. C., Ed.; Kluwer Academic Publishers: Boston, 1992; Vol. C, Table 4.2.6.8, pp 219−222.

(41) Ibers, J. A.; Hamilton, W. C. *Acta Crystallogr.* **1964**, *17*, 781.

(42) *CrystalStructyre 3.7.0*: Crystal Structure Analysis Package; Rigaku and Rigaku/MSC: The Woodlands, Tx, 2000−2005.

(43) Sheldrick, G. M. *SIR 97 and SHELX 97, Programs for Crystal Structure Refinement*; University of Gottingen: Gottingen, Germany, 1997.